Characterization of the Phenanthrene-Tetrachlorophthalic Anhydride (P/TCPA) 1:1 Charge-Transfer Crystal: Spectroscopic and Structural Investigations

J. Krzystek *, J. U. von Schütz, and H. C. Wolf

3. Physikalisches Institut der Universität Stuttgart

R.-D. Stigler and J. J. Stezowski

Institut für Organische Chemie, Universität Stuttgart

Z. Naturforsch. **42 a**, 622–630 (1987); received February 28, 1987

The 1:1 phenanthrene-tetrachlorophthalic anhydride (P/TCPA) charge-transfer complex crystalizes with monoclinic symmetry, space group $P2_1$, with two magnetically inequivalent stacks in the unit cell. The noncentrosymmetric space group is very unusual for CT-complexes. The optical emission spectra at low temperature are characterized by a strong CT phosphorescence and a weak CT fluorescence and delayed fluorescence.

The S_1 band lies at 22 800 ± 100 cm^{-1}, the T_1 band at 21 200 ± 100 cm^{-1}. Above 15 K triplet excitons, moving along the stacks are revealed by ESR. They have a CT character of about 30%, coinciding with that of the shallow X-traps found by ODMR at low temperatures. A further trap, with zero-field-splitting (zfs) parameters of $D = \pm 0.0617$, $E = \mp 0.0116$ cm^{-1} has a much larger CT character of 50% as found in the isolated complex in low-temperature glass [1]. A structural model is proposed.

Key words: Charge-transfer crystal, crystal structure, fluorescence, phosphorescence, triplet excitons.

1. Introduction

Crystals of weak charge-transfer (CT) complexes have attracted considerable attention in recent years due to their particular structure of parallel, infinite stacks of alternating donor and acceptor molecules. As a result of this structure one may expect anisotropy in different crystal properties, such as electronic excitation energy transfer for example. In particular, triplet excitons have been studied in some detail for the dimensionality of their movement, and it is now widely accepted that this movement appears preferably along the stacking direction [2]. Some other characteristics of the triplet exciton have not yet been completely understood. One of them is the dependence of the exciton mobility on the CT character of the excitonic triplet state.

A high CT character of the lowest triplet state of P/TCPA was first postulated by Yu [1], as deduced from ESR results on the isolated complex in a low-temperature glass and the optical emission spectra of the crystal. The aims of this work were therefore:

- to estimate the CT character of the lowest triplet state of the complex in its crystalline form,
- to determine the relation of the CT character with the triplet energy transfer properties. In particular, we hoped to find "self-trapping" phenomena of the triplet excitons, as found in systems with high CT character [3].

As the structure of P/TCPA was unknown, it was determined by single crystal X-ray diffraction methods in an effort to better understand the interrelationships between structure and physical properties.

2. Experimental

2.1 Crystal Preparation

Both phenanthrene and TCPA were extensively zone-refined. Equimolar amounts of the donor and acceptor were dissolved in acetone and the temperature of the solution was slowly lowered. The yellow crystals obtained from the oversaturated solution had an average size of $10 \times 1 \times 0.5$ mm^3, almost all

* On leave from the Institute of Physics, Polish Academy of Sciences, Warsaw, Poland.

Reprint requests to Prof. Dr. H. C. Wolf, 3. Physikalisches Institut der Universität Stuttgart, Pfaffenwaldring 57, D-7000 Stuttgart 80.

0932-0784 / 87 / 0600-0622 $ 01.30/0. – Please order a reprint rather than making your own copy.

of them were, however, twinned. The crystals showed well-developed (100) faces, as determined by Laue X-ray diffraction.

2.2 X-ray Experiments

Diffraction data were obtained from a $1.0 \times 0.5 \times 0.2\ mm^2$ crystal, sealed in a thin-walled glass capillary, with monochromatized MoK_α radiation ($\lambda = 0.71069$ Å) using a Syntex P1 autodiffractometer equipped with a Syntex LT-1 low temperature device which maintained the crystal at ~ 120 K. Lattice parameters were refined [4] with automatically centered 2θ values for 30 reflections ($31.32° \leqq 2\theta \leqq 42.75°$). Intensities were measured for all unique reflections with an ω-scan technique (scan range 0.75°, scan rate 2.0 to 24.0°/min; background measured at each side ($\Delta\omega = 1°$) of the reflection for one half the scan time). Three periodically monitored reference reflections displayed variations of no more than 5% in their intensities during measurement. Data were corrected for Lorentz and polarization effects but not for absorption, $\mu = 6.6\ cm^{-1}$.

The initial model was determined by direct methods (program Shel XS 84 [5], and developed by difference Fourier methods (X-ray program package version of 1976 [6]). Atomic coordinates and anisotropic temperature factors for heavy atoms were refined as were coordinates, found by Fourier techniques, and isotropic temperature factors for H atoms by least-squares techniques. A single scale factor was used. The weighting scheme employed was

$$w = [\sigma^2(F_0) + 0.0065\,|F_0| + 10^{-5}\,|F_0|^2 + 1.8 \times 10^{-5}\,|F_0|^3]^{-1}.$$

Of the 2900 unique reflections measured ($\sin\theta/\lambda \leqq 0.7\ Å^{-1}$), 2748 contributed to the refinement of 301 variables to give $R = 0.032$, $Rw = 0.045$ and σ, the estimated standard deviation of an observation of unit weight, = 0.92.

2.3 Optical Measurements

The optical measurements were made using two Spex 0.2 m double monochromators equipped with a cooled S 20 photomultiplier. An XBO 900 xenon lamp with a regulated intensity served as an excitation source and an Oxford Instruments CF 204 helium-flow cryostate kept the crystal at the desired temperature. The digitalized data were collected by a North Star Horizon computer.

2.4 ODMR Measurements

The ODMR equipment is described in detail in [7]. As an excitation source alternatively a HBO 100 mercury lamp with suitable filters or a helium-cadmium Spectra Physics 185 laser was used.

2.5 ESR Measurements

For the ESR experiments a Varian E109 X-band spectrometer was used.The temperature was controlled by an Oxford Instruments E 900 helium flow cryostat. The excitation was achieved by means of an XBO 1600 xenon lamp with the short-wave radiation being cut off by a 345 nm low-pass filter.

3. Results

3.1 Crystal Structure

The crystal is monoclinic, space group $P2_1$, with $a = 9.102(2)$, $b = 7.063(1)$, $c = 14.504(1)$ Å, $\beta = 95.76(1)°$, $V = 927.75$ Å^3, $Z = 2$, $\varrho_{calc} = 1.66\ g/cm^3$.

The atomic parameters together with isotropic equivalent temperature factors are presented in Table 1 †.

The bonding geometry is presented in Figs. 1 and 2. Bond lengths and bond angles in TCPA are equal (within experimental error) to the values in the neat molecular crystal [9, 10]. Exceptions are the bond lengths from atoms C(7) and C(8) to O(9), where the differences are 0.012 Å and 0.017 Å, respectively. The bond lengths in phenanthrene in the complex are similar to those in the neat molecular crystal [11], especially after the latter were corrected for thermal motion, whereas the bond angles are equal within the experimental error in both structures.

The equation of the mean phase of the phenanthrene molecule in the orthogonal coordinate system a, b, c^* [8] is

$$0.3079\,x + 0.9494\,y - 0.0620\,z = 4.7911\,.$$

† Further structural data can be obtained from the Fachinformationszentrum Energie, Physik, Mathematik GmbH, D-7514 Eggenstein-Leopoldshafen 2 upon quoting the number CSD 52249, the title and the authors of this paper.

Table 1. List of atomic parameters of the complex atoms C(1T) to O(9T) belong to the TCPA molecule atoms C(1) to C(10A) belong to the phenanthrene molecule.

Atom	*X*	*Y*	*Z*	*U*
C(1T)	0.7623(3)	−0.0301(4)	0.3330(2)	0.01324
CL(1T)	0.77500(8)	0.005800	0.45019(5)	0.01877
C(2T)	0.8827(3)	−0.0898(5)	0.2892(2)	0.01337
C(3T)	0.8752(3)	−0.1062(4)	0.1938(2)	0.01413
C(4T)	0.7477(3)	−0.0676(5)	0.1372(2)	0.01481
CL(4T)	0.74158(8)	−0.0796(2)	0.01899(5)	0.02022
C(5T)	0.6226(3)	−0.0155(5)	0.1801(2)	0.01410
CL(5T)	0.45737(7)	0.0209(1)	0.11448(5)	0.01903
C(6T)	0.6297(3)	0.0044(5)	0.2772(2)	0.01395
CL(6T)	0.47622(7)	0.0779(1)	0.32690(5)	0.01660
C(7T)	1.0339(3)	−0.1432(5)	0.3282(2)	0.01726
O(7T)	1.0895(3)	−0.1534(4)	0.4055(2)	0.02306
C(8T)	1.0233(3)	−0.1664(5)	0.1691(2)	0.01665
O(8T)	1.0704(2)	−0.1933(4)	0.0971(2)	0.02384
O(9T)	1.1128(2)	−0.1886(4)	0.2532(2)	0.01968
C(1)	1.0171(3)	0.3197(5)	0.1537(2)	0.01926
H(1)	1.026(5)	0.273(7)	0.083(3)	0.04(1)
C(2)	1.1326(4)	0.2849(5)	0.2193(2)	0.02128
H(2)	1.228(4)	0.255(6)	0.204(3)	0.02(1)
C(3)	1.1153(3)	0.3101(5)	0.3140(2)	0.01993
H(3)	1.197(4)	0.281(5)	0.362(2)	0.009(8)
C(4)	0.9823(3)	0.3724(5)	0.3415(2)	0.01600
H(4)	0.970(4)	0.382(5)	0.411(2)	0.009(8)
C(4A)	0.8605(3)	0.4109(5)	0.2754(2)	0.01436
C(4B)	0.7175(3)	0.4746(4)	0.3013(2)	0.01385
C(5)	0.6903(3)	0.5058(5)	0.3942(2)	0.01796
H(5)	0.750(4)	0.494(7)	0.454(3)	0.019(9)
C(6)	0.5532(3)	0.5665(5)	0.4156(2)	0.02153
H(6)	0.529(6)	0.63(1)	0.479(4)	0.06(2)
C(7)	0.4393(3)	0.5995(5)	0.3452(2)	0.02087
H(7)	0.346(5)	0.634(7)	0.363(3)	0.03(1)
C(8)	0.4627(3)	0.5719(5)	0.2543(2)	0.01745
H(8)	0.387(4)	0.597(6)	0.202(2)	0.016(9)
C(8A)	0.6017(3)	0.5081(5)	0.2300(2)	0.01440
C(9)	0.6250(3)	0.4801(5)	0.1346(2)	0.01718
H(9)	0.536(3)	0.490(5)	0.085(2)	0.003(7)
C(10)	0.7576(3)	0.4203(5)	0.1108(2)	0.01828
H(10)	0.790(4)	0.394(7)	0.044(3)	0.03(1)
C(10A)	0.8791(3)	0.3841(4)	0.1800(2)	0.01445

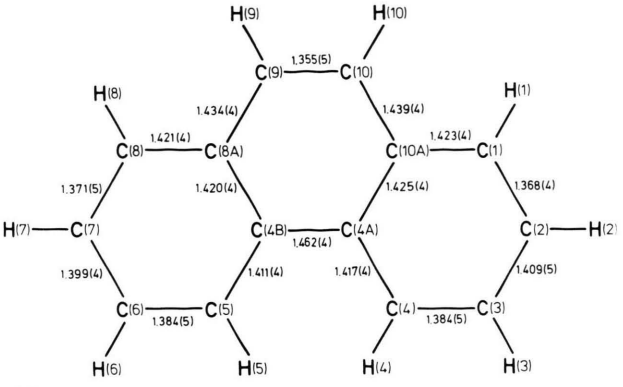

(a)

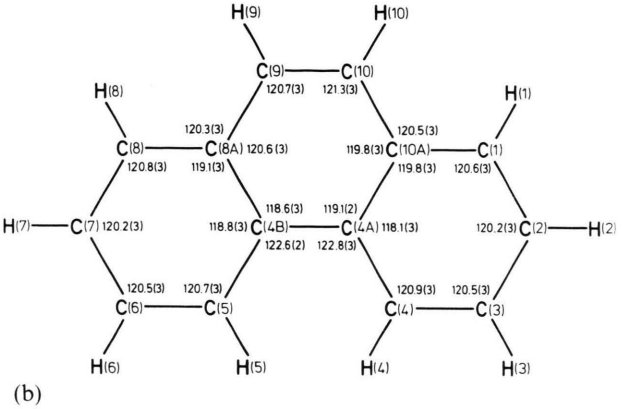

(b)

Fig. 1. Atom numbering, bond lengths in Å (a) and bond angles in degree (b) in phenanthrene.

For TCPA, the standard deviation from the mean plane is 0.018 Å and the equation is

$$0.2870x + 0.9556y - 0.0670z = 1.2975.$$

The mean deviation of the atoms from the plane is 0.004 Å.

The complex forms the usual mixed ...−D−A−D−A... infinite stacks (Fig. 3) with donor and acceptor molecules parallel to each other within 1.3°, and inclined to the *b* axis, the stacking axis by 18.3° (phenanthrene) and 17.1° (TCPA). The intrastack-interplanar distances are depicted in Figure 4. Distances are calculated from centre of molecule to molecular plane; for phenanthrene the centre of the molecular plane is calculated as the arithmetic average of the coordinates of all carbon atoms. That of TCPA is calculated as arithmetic average of the coordinates of atoms C(1T), C(2T), C(3T), C(4T), C(5T), C(6T), C(7T), C(8T), and O(9T), respectively.

There are two stacks in the unit cell, related by the symmetry operator $-x, 1/2+y, -z$. Because of space group symmetry the interplanar interstack angle for phenanthrene molecules is 36.6°; for TCPA molecules this angle is 34.3°. There are only a few close contacts within one stack:

Cl(6T)−C(7) 3.409 Å (symmetry operator $x, 1-y, z$),
Cl(6T)−C(8) 3.583 Å (symmetry operator x, y, z),
O(9T)−C(7) 3.472 Å (symmetry operator $1+x, y-1, z$).

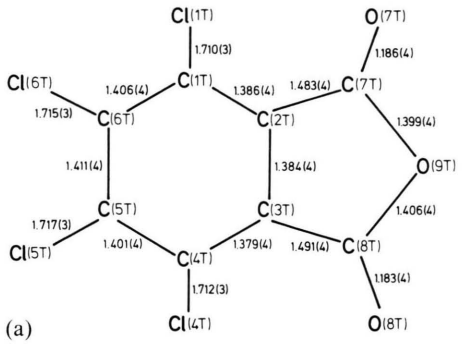

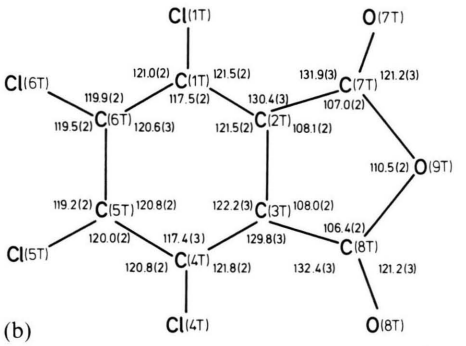

Fig. 2. Atom numbering, bond lengths in Å (a) and bond angles in degree (b) in TCPA.

3.2 Optical Emission

The total emission spectrum of P/TCPA at 4.2 K with excitation above the S_1 band is shown in Figure 5. Under these conditions it consists principally of a long-lived component (lifetime of about 1 s) identified as phosphorescence with the onset at about 21200 cm^{-1}. A small part (about 5% of the integral intensity) of the total emission is short-lived (lifetime about 10 ns) with the onset at about 22800 cm^{-1} and is identified as prompt fluorescence. The separation of the different contributions to the spectrum was achieved by time resolved spectroscopy.

The value of 22800 cm^{-1} corresponds to an absorption edge in the excitation spectra. The intensity ratio of delayed/prompt emission can be changed either by increasing the excitation wavelength or increasing the temperature.

Upon increasing the excitation wavelength the phosphorescence intensity gradually decreases and shifts toward the red. With an excitation below 21200 cm^{-1} no phosphorescence could be observed. On the contrary, the intensity of the fluorescence decreases only slightly, although a red shift is also observed.

Upon increasing the temperature, a similar effect can be achieved, i.e. a red-shift of the phosphores-

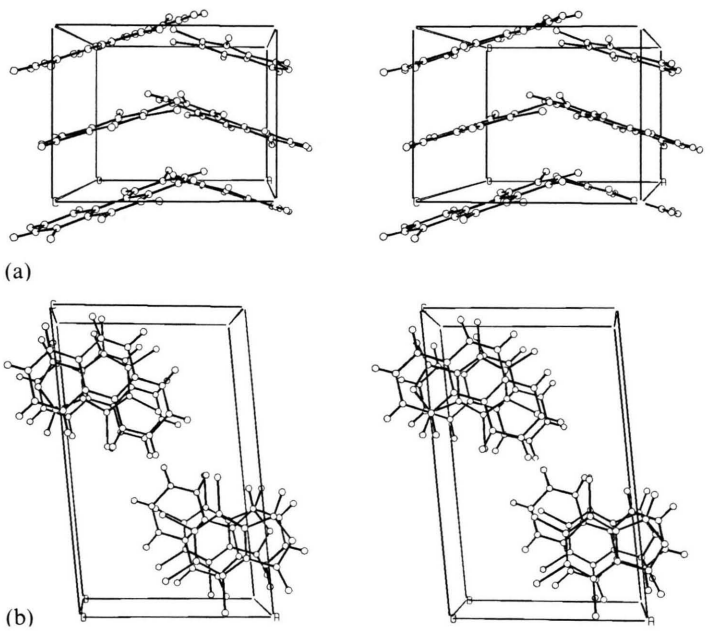

Fig. 3. Stereoscopic projection of the unit cell along the *a* axis (a) and the *b* axis (stacking axis) (b).

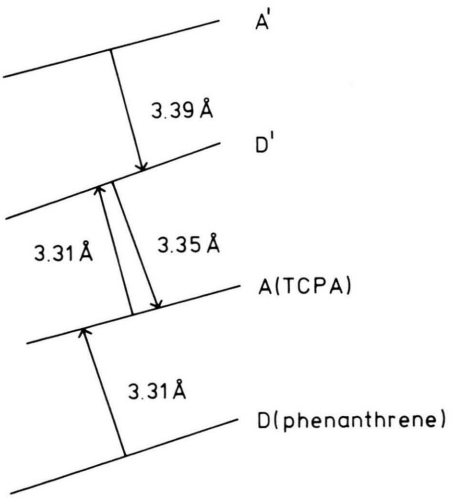

Fig. 4. Scheme of the intrastack interplanar distances.

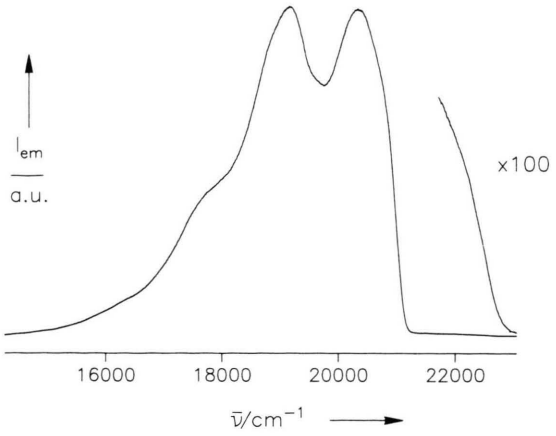

Fig. 5. Total emission spectrum of P/TCPA at 4.2 K. The excitation was at 25 640 cm^{-1}. The emission beginning at 21 200 ± 100 cm^{-1} is phosphorescence overlapping the weak fluorescence with the onset at 22 800 ± 100 cm^{-1}.

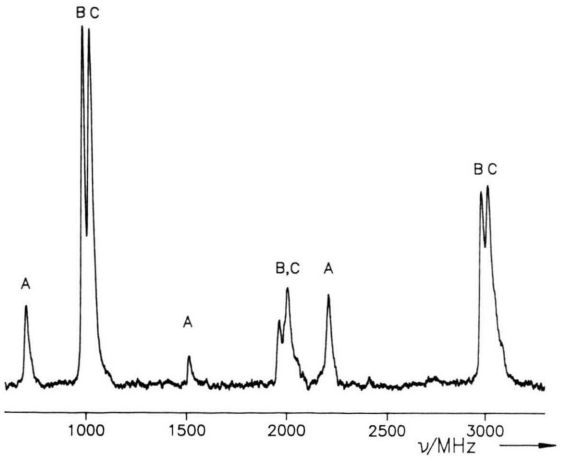

Fig. 6. The ODMR spectrum at 1.2 K monitoring the phosphorescence at 19 300 cm^{-1}, excitation at 24 750 cm^{-1}. The signal at 1948 MHz is artificial, due to a second harmonic generated by the microwave source sweeping through the 974 MHz transition.

cence together with a decrease of its intensity, while the intensity of the fluorescence remains almost constant. The decrease of the delayed emission intensity has an activation energy of 200 ± 50 cm^{-1} between 4.2 and 50 K. At higher temperature (above about 100 K) an additional, very weak component of the emission could be identified, with a lifetime in the ms range and the onset at about 22800 cm^{-1}. This emission may be identified as delayed fluorescence.

3.3 Zero-Field ODMR

The complete ODMR spectrum of P/TCPA at 1.2 K is shown in Fig. 6 using the delayed emission for detection. The spectrum consists of at least 9 lines, which can be associated with 3 different triplet states. The assignment of particular signals to the correponding set was achieved by varying the excitation wavelength, temperature (between 1.2 and 4.2 K) and by means of double resonance (EEDOR) experiments. The three triplet states will subsequently be named A, B and C. At 1.2 K and with the excitation at 404 nm (above the S_1 band) the states B and C give very strong signals (visible by eye). Warming the crystal to 4.2 K causes the signals of state C to disappear completely, while the A signals become stronger in relation to the B signals. Finally, changing the excitation to the 441 nm line of the He–Cd laser leaves only the A signals present, even at 1.2 K.

Table 2. Zero-field-parameters of the triplet states observed by the ODMR (experimental error 0.0001 cm^{-1}).

Parameter	State		
	A	B	C
$\|D\|$ (cm^{-1})	0.0617	0.0828	0.0834
$\|E\|$ (cm^{-1})	0.0116	0.0162	0.0168

The zfs parameters of the three states observed in the ODMR spectra are shown in Table 2. Anticipating the discussion, state A is a deep trap, states B and C have magnetic properties close to that of the exciton (X-traps).

3.4 ESR

The ESR spectrum of P/TCPA was recorded in the temperature range between 3.8 and about 250 K. At 3.8 K the spectrum is rather complicated, consisting of 2 sets of 4 pairs of signals for an arbitrary orientation of the crystal relative to the magnetic field (Figure 7). One set concerns the strong signals, the other the weaker ones, which are in Fig. 7 only visible in the high field transitions. By increasing the temperature or changing the excitation source from the XBO lamp to the He–Cd laser it was possible to attribute the signals to two distinct states. As shown later, the strong signals are identical with the state A (deep trap), the weak ones with the fine structure of B/C. In order to simplify the

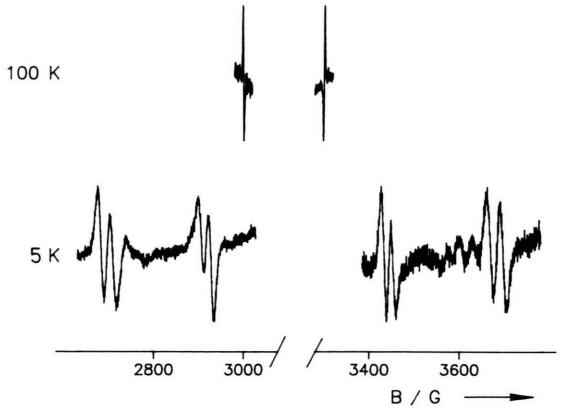

Fig. 7. The ESR spectrum at two temperatures for two arbitrary orientations of the crystal relative to the magnetic field. The strong signals at 5 K originate from the A state, only traces of the weaker B state signals are visible at high field. In order to achieve the best signal to noise ratio at 100 K the crystal was positioned so that the 4 pairs of signals overlap, yielding only one pair. Signal averaging (20 times) was nevertheless necessary.

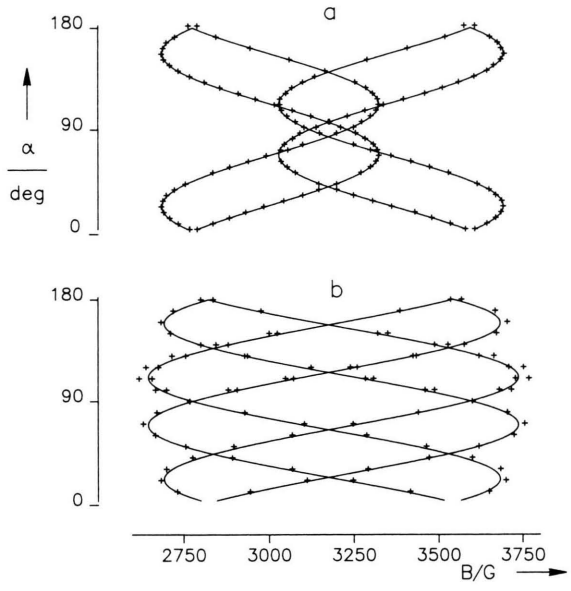

Fig. 8. The angular dependence of ESR signals at 20 K. The crystal was rotated in the ac plane (a) and the ab plane (b). The crosses represent experimental points while the curves were calculated using the zfs parameters in the text. The appearance of two sets of curves in Fig. (a) and the doublet structure in some orientations in Fig. (b) is caused by crystal twinning. $\nu_{rf} = 8.990$ GHz.

observed ESR spectrum, in subsequent experiments the temperature was kept at or above 20 K, where the trap states B/C are no longer detectable.

Therefore the spectrum at 20 K consists only of 4 pairs of signals, each about 10 G wide (depending on the crystal orientation) and Gaussian-shaped. The appearance of 4 pairs of signals instead of 2 pairs as expected from the crystal structure is caused by crystal twinning. In fact practically all the crystals examined were twinned.

The angular dependence of the ESR signals in two rotation planes is shown in Figure 8. The zfs parameters D and E were obtained by a numerical fit to the experimental curves. The parameters are:

$$D = \pm 0.0615(2), \quad E = \mp 0.0116(2)\ \mathrm{cm}^{-1},$$

which identifies without doubt the state observed by ESR as identical with the A state recorded by the ODMR.

The orientation of the two zfs tensors (neglecting the effect of twinning) is the following: the principal tensor axes corresponding to the largest splitting of the pairs of ESR signals (conventionally the z axes of the tensors) point in the directions $+68°$ and $-68°$ from the stack axis, respectively, and also $68°$ from the c axis. The second largest principal axes of the tensors (x axes) form angles of $+22°$ and $-22°$ with the stack axis, respectively (the experimental error is $\pm 2°$). This means that the tensor principal axes are within $4°$ parallel to the molecular axes of phenanthrene: the z axis is parallel to the long in-plane axis of phenanthrene and the x axis to the out-of-plane axis.

Upon increasing the temperature beyond 30 K the signals attributed to the A state gradually disappear. Above 15 K a new set of 4 pairs of signals emerge, very different in their parameters from those observed at low temperature. They are less than 2 G wide, spin-polarized and saturate at microwave power levels at least 2 orders of magnitude higher than those of the previously described signals. Their intensity is very low and does not change until about 250 K, when they gradually disappear. Their linewidth is constant above 80 K but is thermally activated (narrowed) between 15 and 80 K with an activation energy of 20 cm^{-1}.

Due to the very low intensity of the signals their angular dependence can only be followed in a very narrow angular range ($\pm 40°$ from the c axis). Therefore it was not possible to calculate precisely the zfs parameters of this new state. We tried to estimate them by extrapolation of the observed

angular dependence into the region where the signals disappear (it should correspond to the orientation of the phenanthrene molecule in the crystal). As the result we obtained the following zfs parameters $D \sim 0.090 \pm 0.010\ \mathrm{cm}^{-1}$, $E \sim 0.017 \pm 0.005\ \mathrm{cm}^{-1}$.

These parameters are by approximately 50% larger than those of the A state but close to those of the B and C states. We will subsequently call this state the exciton state.

4. Discussion

4.1 The Energy and Character of the Electronic States

The onset of the prompt fluorescence at 22800 $\pm$ 100 cm^{-1} approximately determines the position of the lowest singlet state of the crystal. This is confirmed by the excitation spectra, where the same energy value corresponds to the steepest slope of the absorption edge. It should be noted, however, that this edge is not very sharp, and there is considerable absorption present below the S_1 band. This leads to a relatively strong emission when the crystal is excited below the S_1 band and can be explained by the presence of a considerable number of singlet traps. This has been observed in many other CT crystals [12, 13] but has not been explained satisfactorily. The lack of any structure in the 0–0 region of the fluorescence indicates a large CT character in the S_1 state, as is the case in most CT crystals.

The position of the lowest triplet band can be estimated from the onset of the phosphorescence at very low temperature (here 4.2 K) at 21200 $\pm$ 100 cm^{-1}. This is in good agreement with the observation of a zero-phonon transition in the triplet excitation spectrum at 21162 cm^{-1} [14]. The S_1-T_1 energy gap is therefore only about 1600 cm^{-1}, and is indicative for a medium CT character of the T_1 state (see below).

An interesting feature of the P/TCPA crystal is an unusual intensity ratio of fluorescence to phosphorescence at low temperature. In fact, it is very hard to detect any prompt fluorescence at 1.2 K. Apparently there is a very efficient intersystem crossing between the S_1 and T_1 states. This efficiency is not limited to the band-band transition but is also found in the traps: exciting below the S_1 band (this means into the numerous singlet traps) one still obtains a very strong phosphorescence from the triplet traps. Such a coordination of singlet and triplet traps has already been noticed in other CT crystals [12].

The charge-transfer character of each of the states A, B/C can be roughly estimated by comparing them with the corresponding parameters of the isolated phenanthrene molecule (the TCPA molecule with its lowest triplet state at about 2000 cm^{-1} above that of phenanthrene [15, 16] does not need to be considered in the first approximation). The molecular parameters of phenanthrene are

$$D = \pm\, 0.1004, \quad E \mp = 0.0466\ \mathrm{cm}^{-1}\ [17].$$

In order to compare them with those of the complex, however, they have to be re-defined in the convention used in the ODMR (where E has to be smaller than 1/3 D). In the ODMR convention their values are then

$$D = \pm\, 0.1201, \quad E = \mp\, 0.0269\ \mathrm{cm}^{-1}.$$

Using the standard formula

$$C_{CT}^2 = \frac{D(\mathrm{AD}^*) - D_{\mathrm{exp}}}{D(\mathrm{AD}^*) - D(\mathrm{A}^-\,\mathrm{D}^+)}\ [18]$$

and neglecting the zfs parameters of the hypothetical ionic form of the complex, one obtains the values c_{CT}^2 to be about 50% for the deep trap A and about 30% for the states B and C (the difference between the latter ones is very small) as well as for the excitonic state.

4.2 Triplet Exciton Dynamics

In view of the fact that most of the emission at very low temperature is long-lived phosphorescence originating from defects, it is not surprising that the ODMR signals observed on this emission have all the characteristics of the trap signals: linewidths of 12 MHz, inhomogenous broadening and time response in the order of one second. This concerns all the states A, B, and C detected by the ODMR technique. The same conclusion can be drawn from the ESR experiments conducted between 3.8 and about 30 K (the two observed states in the ESR spectrum in this temperature range can be identified by their zfs parameters as trap A and B states). The depth of the three trap states can be estimated from

the temperature dependence of the ODMR and ESR intensity: trap A is $200 \pm 50\ cm^{-1}$ deep, trap C $\sim 10\ cm^{-1}$ deep (it disappears in the ODMR spectrum between 1.2 and 4.2 K), and the depth of the trap B lies between these values. From the trap depths it can be concluded that trap C represents the least distorted state in comparison with the excitonic state of the crystal, while trap A is the most distorted one. A measure of the trap A distortion can be taken from the orientation of its zfs tensor relative to the undisturbed molecular axes: the difference in the case of the out-of-plane axis is $4 \pm 2°$ (the assumption has to be made that the molecular and the zfs principal axes coincide). All of the states, however, are CT states as proved by the broad and only weakly structured phosphorescence emitted from them.

Elevating the temperature leads to a thermal detrapping of the triplet energy starting from the most shallow trap C. A "pumping effect" of the excitons can be observed both in the optical emission and in the ODMR spectra; that means the excitons are re-captured on deeper traps resulting in a red shift of the phosphorescence and a change of the relative intensities of the ODMR signals. At least some fraction of them, however, is activated to the excitonic triplet band. This can be deduced from the appearance of the delayed fluorescence in the emission. It is confirmed even more by the appearance of the excitonic ESR signal at about 15 K. The characteristics of mobile excitons: Linewidths of less than 2 G and strong spin polarization are given in the range between 80 and 250 K.

An intriguing question is the CT character of the excitons, as, unlike defects, they represent the general properties of the crystal. The answer to this question cannot be given precisely, but one can accept the view that the CT character of the excitons is very similar to that of the trap C, because the zfs parameters of both are more or less the same, and trap C is the most shallow of all, representing therefore the least distorted trap state in the crystal. The CT character of the excitons can then be estimated as being not larger than 30%.

This small percentage of CT explains that the effect of "self-trapping", as manifested by the temperature dependence of the excitonic linewidth, is only weakly pronounced. Thermal activation is therefore accessible at much lower temperatures than in case of biphenyl/TCNB [3] or fluorene/TCNB [7], crystals with significant CT-character.

The observation of 2 pairs of excitonic ESR signals (neglecting the effect of crystal twinning) points to their movement preferably along the stacks. This observation is similar to that made in the crystals P/PMDA [2] and A/TCNB [19], which are also characterized by the existence of two magnetically inequivalent stacks, at least at low temperature.

The low CT character of the excitonic state as well as of the X-traps B and C is somewhat surprising because of the earlier results on the isolated complex in low-temperature glass [1]. CT complexes in glasses, however, are isolated D*A pairs with defined charge-transfer between only two partners. In a mixed-stack crystal an excited donor has at least two neighbours, AD*A, and such a trimer can have a different degree of charge transfer. For the trap A, which has the zfs parameters very close to the isolated complex, the following configuration is therefore suggested: AD*Y, where Y is either a vacancy or a substitutionally built in impurity in an acceptor position. D* is coupled stronger to A therefore, which corresponds to a higher CT-character as observed experimentally.

Acknowledgements

The financial support of Stiftung Volkswagenwerk is gratefully acknowledged. One of us (J.K.) thanks the Grimmke Stiftung (Düsseldorf) and the Max-Planck-Gesellschaft for grants making his stay in Stuttgart possible. The crystals were grown by W. Tuffentsammer in the Kristallabor/Stuttgart. Inspiring discussions with N. Karl, W. Mühle, and H. Port are also acknowledged.

[1] C.-T. Yu, Ph.D. thesis, Washington University, St. Louis 1979.
[2] C. P. Keijzers and D. Haarer, J. Chem. Phys. **67,** 925 (1977).
[3] H. Möhwald and E. Sackmann, Chem. Phys. Letters **21,** 43 (1973).
[4] Program P3, Nicolet Corporation, Version 3/81.
[5] G. M. Sheldrick, Shel X84 (test version), Institut für Anorganische Chemie der Universität Göttingen, implemented on the CRAY-1M computer of the Rechenzentrum der Universität Stuttgart by Dipl.-Chem. H. W. Pöhlmann.
[6] J. M. Stewart, P. A. Machin, C. W. Dickinson, H. L. Ammon, H. Flack, and H. Heck, X-ray version of 1976, Technical Report TR-446. Computer Science Center, University of Maryland, College Park, Maryland, USA.
[7] W. Mühle, J. Krzystek, J. U. von Schütz, H. C. Wolf, R.-D. Stigler, and J. J. Stezowski, Chem. Physics **108,** 1 (1986).
[8] V. Schomaker, J. Wäser, R. E. Marsh, and G. Bergman, Acta Cryst. **12,** 600 (1959).
[9] D. E. S. Gowda and R. Rudman, Acta Cryst. **B 38,** 2842 (1982).
[10] T. Uchida, H. Nakano, and K. Kozowa, Acta Cryst. **B 38,** 2963 (1982).
[11] M. J. Kai, Y. Okaya, and D. E. Cox, Acta Cryst. **B 27,** 26 (1971).
[12] J. U. von Schütz, D. Burger, R. Krauss, W. Mühle, and H. C. Wolf, J. Luminesc. **24/25,** 467 (1981).
[13] F. C. Bos and J. Schmidt, Mol. Phys. **58,** 561 (1986).
[14] S. Käsdorf, Diplomarbeit, Stuttgart University, 1981.
[15] S. Iwata, J. Tanaka, and S. Nagakura, J. Chem. Phys. **47,** 2203 (1967).
[16] J. Langelaar, R. P. H. Retschnick, and G. J. Hoitink, J. Chem. Phys. **54,** 1 (1971).
[17] R. W. Brandon, R. E. Gerkin, and C. A. Hutchinson, J. Chem. Phys. **41,** 3717 (1964).
[18] H. Möhwald and E. Sackmann, Z. Naturforsch. **29a,** 1216 (1974).
[19] A. M. Ponte Goncalves, Chem. Physics **19,** 397 (1977).